Light Neutralino Dark Matter In Gaugino Non-Universal Models

Nicolao Fornengo

Department of Theoretical Physics, University of Torino and INFN - Sezione di Torino, via P. Giuria 1, 10125 Torino, Italy, email: fornengo@to.infn.it, web: www.to.infn.it:/~fornengo and www.astroparticle.to.infn.it

Summary. We [1] examine the cosmology and the astrophysical signals produced by neutralino dark matter in the frame of an effective MSSM model without gaugino-mass unification at a grand unification scale. As a consequence of the recent data on precision cosmology, we can set an absolute lower bound of 6 GeV on the neutralino mass. This limit changes to 25 GeV if the pseudoscalar higgs is heavier than 180 GeV. The light neutralinos allowed in this class of supersymmetric models provide quite sizeable direct detection rates. We show how they compare to the direct detection esperimental sensitivites: the predicted rates are largely compatible with the annual-modulation data of the DAMA Collaboration; the comparison with the upper bounds of the CDMS and EDELWEISS Collaborations shows that limits for neutralino masses below 25–30 GeV can be set for a standard isothermal halo. As for the annihilation signals, we find that only low–energy antiprotons and antideuterons are potentially able to set constraints on very low–mass neutralinos, below 20–25 GeV. The gamma–ray signal requires significantly steep profiles or substantial clumpiness in order to reach detectable levels. The up-going muon signal at neutrino telescopes is largely below experimental sensitivities for the neutrino flux coming from the Sun, while for the flux from the Earth an improvement of about one order of magnitude in experimental sensitivities with a low energy threshold can make accessible neutralino masses close to O, Si and Mg masses, for which resonant capture is operative.

1 Supersymmetry and gaugino non–universality

A typical assumption of supersymmetric models is the unification condition for the three gaugino mass parameters $M_{1,2,3}$ at the GUT scale: $M_1 = M_2 = M_3$. This hypothesis implies that at the electroweak scale $M_1 \simeq 0.5\ M_2$. Under this unification condition the bound on the neutralino mass is determined to be $m_\chi \gtrsim 50$ GeV. This is derived from the experimental lower bound on the chargino mass (which theoretically depends on M_2 but not on M_1) determined at LEP2: $m_{\chi^\pm} \gtrsim 100$ GeV. By allowing a deviation from gaugino–universality, the neutralino can be lighter than in the gaugino–universal models when $M_1 \equiv R\ M_2$, with $R < 0.5$. In this case current data from accelerators do not set an absolute lower bound on m_χ.

[1] Report on the work done in collaboration with A. Bottino, F. Donato, S. Scopel.

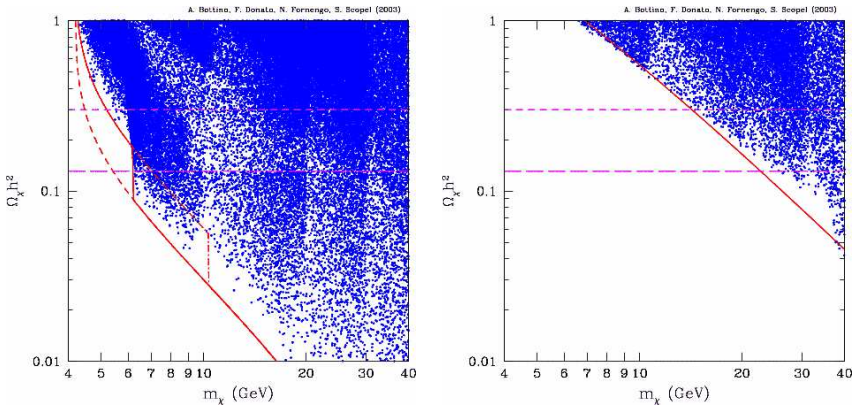

Fig. 1. Neutralino relic abundance $\Omega_\chi h^2$ as a function of the neutralino mass m_χ. LEFT: The solid curve denotes the analtytical lower bound for the relic abundance in the gaugino non–universal MSSM calculated for $T_{\rm QCD} = 300$ MeV, while the dashed and dot-dashed curves refer to the representative values $T_{\rm QCD} = 100$ MeV, $T_{\rm QCD} = 500$ MeV, respectively. The two horizontal lines denote two representative values for the maximal amount of CDM in the Universe: $\Omega_{\rm CDM} h^2 = 0.3$ (short-dashed line) and $\Omega_{\rm CDM} h^2 = 0.131$ (long-dashed line). The scatter plot is obtained by a full scanning of the supersymmetric parameter space. RIGHT: The solid curve denotes the analtytical lower bound for the relic abundance in the gaugino non–universal MSSM calculated when the pseudoscalar higgs is heavy. $T_{\rm QCD}$ is set equal to 300 MeV. The scatter plot is obtained by a full scanning of the supersymmetric parameter space with $m_A > 300$ GeV.

We consider here an extension of the MSSM which allows for a deviation from gaugino–mass universality by the introduction of the parameter R, varied here in the interval: $(0.01 \div 0.5)$ [1, 2, 3, 4]. This range for R implies that the accelerator lower bound on the neutralino mass can be moved down to few GeV for $R \sim 0.01$. The ensuing light neutralinos have a dominant bino component; a deviation from a pure bino composition is mainly due to a mixture of $\tilde{B}$ with $\tilde{H}_1^\circ$ [1, 2, 3]. Notice that our range of R includes also the usual model with gaugino–mass universality.

In the following we will discuss both the cosmology and different kinds of direct and indirect detection rates of the light relic neutralinos arising in this class of supersymmetric models. For a more detailed analysis of all these topics, as well as for a more thorough list of relevant references, see Refs. [1, 2, 3, 4].

2 Cosmology of light neutralinos

In the class of models we are considering here, the neutralino relic abundance $\Omega_\chi h^2$ for very light neutralinos is dominated by two competing annihilation

diagrams [1, 2]: annihilation into a $\bar{b}b$ pair, proceeding through the exchange of the pseudoscalar higgs A, and annihilation into a $\bar{\tau}\tau$ pair, via stau exchange. The mixture of the dominant bino component with the subdominant, but not negligible higgsino amplitude [1, 2, 3], provides sizable yukawa–type interactions between neutralinos and higges: when the A boson is relatively light this makes the annihilation cross section into $\bar{b}b$ the dominant channel. The ensuing relic abundance is a decreasing function of the neutralino mass and it is large for light neutralinos, largely in excess of the cosmological upper bound on the cold dark matter (CDM) content of the Universe [1, 2]. The recent data on the cosmic microwave background [5, 6, 7] and other astrophysical determinations [8, 9] provide stringent limits on the cold dark matter (CDM) content of the Universe: these limits [5] allow us to set an absolute lower bound on the neutralino mass of 6 GeV [2], as shown in the left panel of Fig. 1 [10]. When the A mass is large, the relic abundance is overall larger and determined by the $\bar{\tau}\tau$ pair annihilation: in this case, as shown in the right panel of Fig. 1, a lower limit of about 25 GeV is obtained [2, 11, 12].

3 Searches for relic light neutralinos

Relic neutralinos which act as CDM in the halo of our Galaxy can be searched for by means of different techniques: direct searches rely on the possibility to detect the recoil energy of nuclei in low–background detectors, which neutralinos scatter off; indirect techniques look for self–annihilation products: neutrinos, photons, antimatter.

3.1 Direct detection

The relevant quantity in direct detection is the neutralino–nucleon scattering cross section $\sigma_{\rm scalar}^{\rm (nucleon)}$, multiplied by the factor ξ which defines the fractional amount of neutralinos as dark matter components of the galactic halo. As usual, the fraction ξ is defined in terms of the calculated neutralino relic abundance as: $\xi = \min[1, \Omega_\chi h^2/(\Omega_\chi h^2)_{\rm min}]$, where $(\Omega_\chi h^2)_{\rm min}$ defines the minimal value of the neutralino relic abundance below which we cannot accept that all the galactic DM is made of neutralinos: we have set $(\Omega_\chi h^2)_{\rm min} = 0.095$ [1, 3].

When neutralinos are light, with a mass close to their lower limit established in the previous Section, also the higgs masses are light [1, 3]: in this case not only the relic abundance, but also the scattering cross section is dominated by higgs exchange (in this case, by the light scalar higgs h). The consequence is that $\sigma_{\rm scalar}^{\rm (nucleon)}$ is sizeable, with peculiar properties [1, 3] which constrain the values of $\sigma_{\rm scalar}^{\rm (nucleon)}$ to lie in a very narrow range [1, 3]: the upper bound on $\sigma_{\rm scalar}^{\rm (nucleon)}$ is set by the experimental lower limit on the higgs mass; the lower limit is a consequence of the upper bound on the neutralino

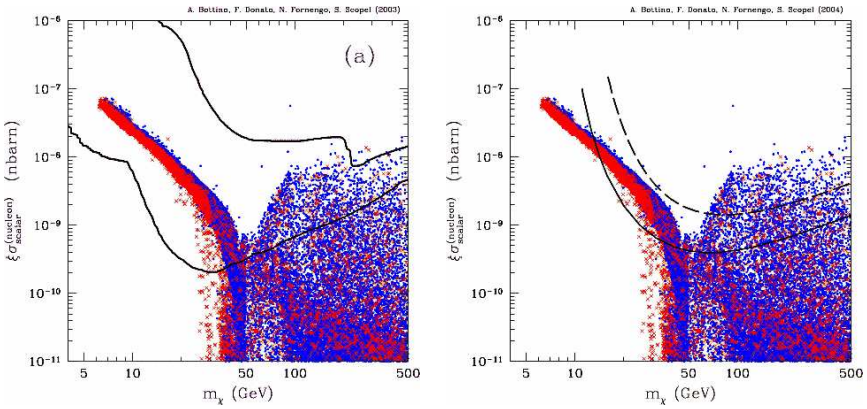

Fig. 2. Scatter plot of $\xi\sigma^{(\mathrm{nucleon})}_{\mathrm{scalar}}$ versus m_χ. Crosses (red) and dots (blue) denote neutralino configurations with $0.095 \leq \Omega_\chi h^2 \leq 0.131$ and $\Omega_\chi h^2 < 0.095$, respectively. LEFT: The curves delimit the DAMA region where the likelihood-function values are distant more than 4σ from the null (absence of modulation) hypothesis [13]; this region is the union of the regions obtained by varying the WIMP DF over the set considered in Ref. [14]. RIGHT: The solid and the dashed lines are the experimental upper bounds given by the CDMS [15] and the EDELWEISS [16] Collaborations, respectively, under the hypothesis that galactic WIMPs are distributed as a cored isothermal sphere with a standard set of astrophysical parameters.

relic abundance, which is strongly correlated to $\sigma^{(\mathrm{nucleon})}_{\mathrm{scalar}}$ in this class on gaugino non–universal models [1, 3]. We see in the left panel of Fig. 2 that the predicted rates are largely compatible with the annual-modulation data of the DAMA Collaboration [13], which takes into account a very large set of possible halo shapes [14]. The comparison with the upper bounds of the CDMS [15] and EDELWEISS [16] Collaborations, which are reported only for an isothermal halo with a local DM density of 0.3 GeV cm^{-3}, shows that in this case limits for neutralino masses below 25–30 GeV can be set: for more general halos, the limits imposed by these experiments may change significantly. For instance, while CDMS would allow to impose a lower limit of about 25 GeV on the neutralino mass in the case of the standard isothermal halo, when the uncertainty on the values of the local density is considered [14], only a fraction of the supersymmetric configurations at low neutralino masses are excluded and no lower limit on m_χ is determined. In any case, direct detection is a very sensitive probe for the light neutralinos of gaugino non–universal supersymmetric models, the most sensitive together with antiprotons and antideuterons searches discussed in the next Section.

3.2 Indirect detection at neutrino telescopes

Indirect evidence for WIMPs in our halo may be obtained at neutrino telescopes by measurements of the upgoing muons, which would be generated

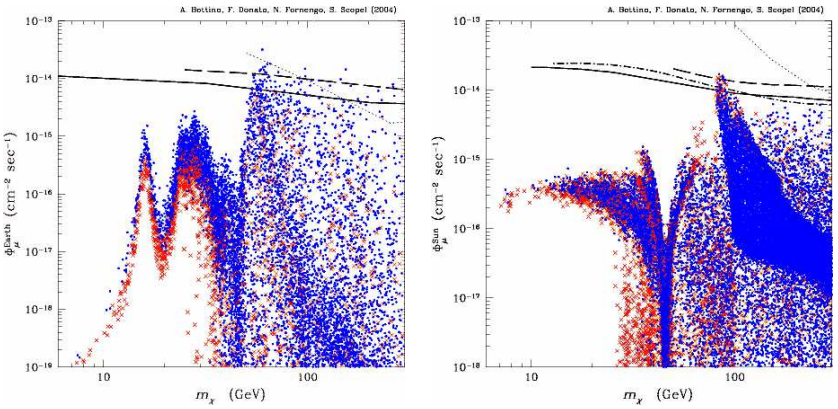

Fig. 3. Scatter plot of the flux of upgoing muons as a function of the neutralino mass. Crosses (red) and dots (blue) denote neutralino configurations with $0.095 \leq \Omega_\chi h^2 \leq 0.131$ and $\Omega_\chi h^2 < 0.095$, respectively. LEFT: Signal from the Earth; the solid, dashed and dotted lines denote the experimental upper limits from SuperKamiokande [17], MACRO [18] and AMANDA [19], respectively. RIGHT: Signal from the Sun; the solid, dashed, dot-dashed and dotted lines denote the experimental upper limits from SuperKamiokande [17], MACRO [18], Baksan [20] and AMANDA [19], respectively.

by neutrinos produced by pair annihilation of neutralinos captured and accumulated inside the Earth and the Sun [4]. The left panel of Fig. 3 shows the expected upgoing muon flux for muon energies above 1 GeV, compared to present experimental upper bounds. For $m_\chi \lesssim 40$ GeV the signal from the Earth presents several peaks due to neutralino resonant capture on Oxygen, Silicon and Magnesium. Apart from the resonances, the predicted flux of light neutralinos is always very small and difficult to be accessed by experimentally. [4]. In the right panel of Fig. 3 we show the up-going muon flux expected from the Sun. Also in this case the signal level turns out to be suppressed for $m_\chi \lesssim 50$ GeV [4] as compared to what is obtained at higher masses. We conclude that investigations of light neutralinos by up-going muons from the Sun do not provide favourable prospects.

3.3 Gamma rays in space

The flux of gamma–rays produced by neutralino self–annihilation inside the galactic halo is potentially a promising tool of investigation. In fig. 4 we show the signal from the galactic center for two different photon energies in the range of EGRET data and for a NFW [22] density profile with a core radius of 0.01 pc. The angular field of view has been chosen to match the EGRET resolution [21]. We clearly see that the small mass range is the most favourable sector of the supersymmetric model for this kind of signal (as is for all the signals which come from neutralino annihilation in the Galaxy).

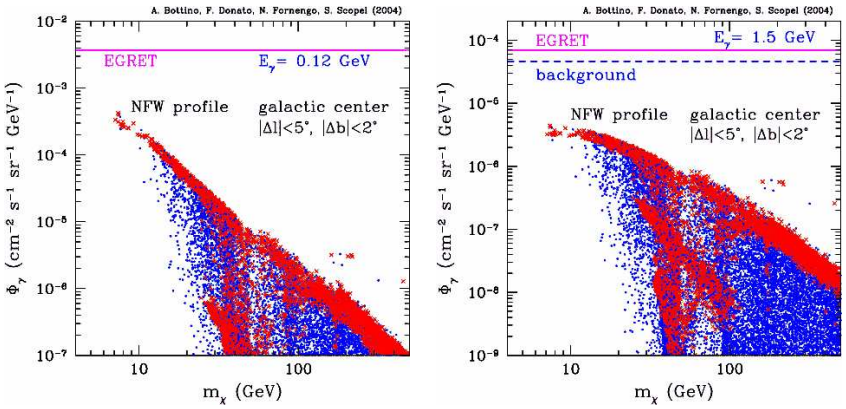

Fig. 4. Scatter plot of the gamma–ray flux from the galactic center inside the angular region $|\Delta l| \leq 5^\circ$, $|\Delta b| \leq 2^\circ$ for a NFW matter density profile. Crosses (red) and dots (blue) denote neutralino configurations with $0.095 \leq \Omega_\chi h^2 \leq 0.131$ and $\Omega_\chi h^2 < 0.095$, respectively. LEFT: Flux calculated at $E_\gamma = 0.12$ GeV; the horizontal line shows the gamma–ray flux measured by EGRET [21], assumed to be compatible with the estimated background [21]. RIGHT: Flux calculated at $E_\gamma = 1.5$ GeV; the solid horizontal line shows the gamma–ray flux measured by EGRET [21], the dashed line is an estimate of the gamma–ray background [21].

Nevertheless, the predicted signal is at least one order of magnitude smaller than the detected flux [4]. In the case of steeper dark matter density profiles, like in the case of the Moore *et al.* shape [23], gamma–ray studies could access the signal produced by neutralinos in the mass range below 10–20 GeV [4]. For cored isothermal halos, the predicted fluex are one order of magnitude smaller the the ones shown in Fig. 4 [4]. Fig. 5 shows that the EGRET excess [21] observed in the energy range above 1 GeV could be explained by light neutralinos in the 30–40 GeV mass range with a DM overdensity factor of about 30 with respect to a NFW profile [4].

3.4 Antimatter in space: antiprotons and antideuterons

Annihilation of neutralinos in the galactic halo may lead also to the production of antiprotons and antideuterons [24] (as well as positrons, which are not considered here). Once antiprotons or antideuterons are produces, they undergo diffusion and energy losses inside the galactic halo before reaching the Earth [25]. For these reason, this kind of signals are less sensitive to the actual dark matter density profile, since they do not significantly probe the central parts of the galactic halo, where the various halo shapes mostly differ. However, uncertainties in the modelling of propagation and diffusion instroduce large uncertainties. This has been thoroughly analyzed for the antiproton signal in Ref. [25]. These uncertainties somehow limit the capabilities of the antiproton signal [25], as it can be seen in Fig. 6. However, especially for

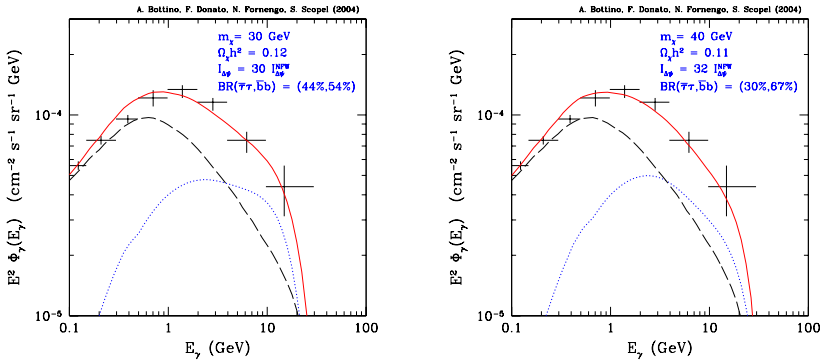

Fig. 5. Gamma–ray spectra $\Phi_\gamma(E_\gamma)$, multiplied by E_γ^2, from the galactic center inside the angular region $|\Delta l| \leq 5^\circ$, $|\Delta b| \leq 2^\circ$, as functions of the photon energy. LEFT: The dotted line is the spectrum for a neutralino with mass $m_\chi = 30$ GeV, calculated for a density profile with a factor 30 of enhancement with respect to the NFW case; the dashed line is the gamma ray background calculated in Ref. [21], reduced by 10%; the solid line is the total flux, sum of the supersymmetric signal and the background; the experimental points are the EGRET data [21]. RIGHT: The same, for $m_\chi = 40$ GeV and for a density profile with a factor 32 of enhancement with respect to the NFW case. The numbers quoted in the legend inside parentheses denote the values of the neutralino annihilation branching ratios into $\bar{b}b$ and $\bar{\tau}\tau$.

neutralinos lighter than 20 GeV, antiprotons represent a potentially relevant probe.

Very promising is the antideuteron signal [24], shown in Fig. 7. The full neutralino mass range below 40 GeV could be probed by antideutrons searches in space

References

1. A. Bottino, N. Fornengo, S. Scopel, Phys. Rev. D **67**, 063519 (2003).
2. A. Bottino, F. Donato, N. Fornengo, S. Scopel, Phys. Rev. D **68**, 043506 (2003).
3. A. Bottino, F. Donato, N.Fornengo, S. Scopel, Phys. Rev. D **69**, 037302 (2003).
4. A. Bottino, F. Donato, N.Fornengo, S. Scopel, Phys.Rev. D **70**, 015005 (2004).
5. D.N. Spergel et al. (WMAP), Astrophys.J.Suppl. **148**, 175 (2003).
6. T.J. Pearson et al. (CBI), Astrophys. J. **591**, 556 (2003)
7. C.L. Kuo et al. (ACBAR), Astrophys. J. **600**, 32 (2004).
8. W.J. Percival et al., MNRAS **327**, 1297 (2001).
9. R.A.C. Croft et al., ApJ **581**, 20 (2002); N.Y. Gnedin and A.J.S. Hamilton, MNRAS **334**, 107 (2002).

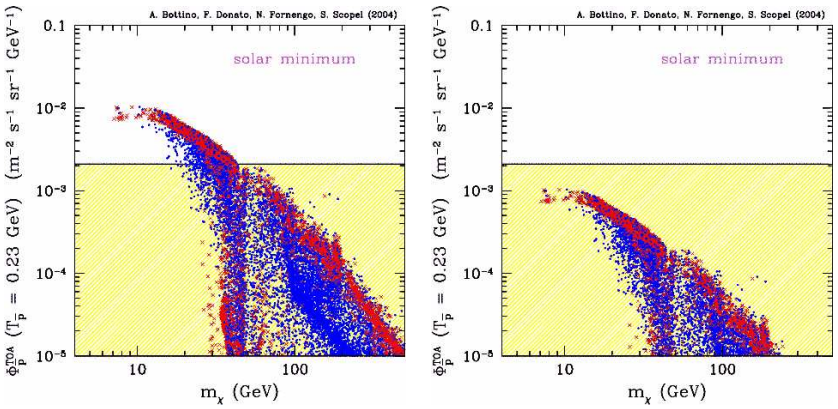

Fig. 6. Scatter plot of the antiproton flux at kinetic energy $T_{\bar{p}} = 0.23$ GeV as a function of the neutralino mass. A spherical isothermal dark matter density profile has been used. The solar modulation is calculated at the phase of solar minimum. Crosses (red) and dots (blue) denote neutralino configurations with $0.095 \leq \Omega_\chi h^2 \leq 0.131$ and $\Omega_\chi h^2 < 0.095$, respectively. The shaded region denotes the amount of primary antiprotons which can be accommodated at $T_{\bar{p}} = 0.23$ GeV without entering in conflict with the experimental BESS data [26, 27] and secondary antiproton calculations [28]. LEFT: The best–fit set of the astrophysical parameters which govern cosmic ray propagation is used. RIGHT: The astrophysical parameters which provide the most conservative antiproton fluxes are used.

10. For older determinations, see: K. Griest and L. Roszkowski, Phys. Rev. D **46**, 3309 (1992); A. Gabutti, M. Olechowski, S. Cooper, S. Pokorski and L. Stodolsky, Astrop. Phys. **6**, 1 (1996); V. A. Bednyakov, H. V. Klapdor–Kleingrothaus and S. G. Kovalenko, Phys.Rev. D **55**, 503 (1997).
11. G. Bélanger, F. Boudjema, A. Pukhov and S. Rosier–Lees, *Proceedings of SUSY02*, Hamburg, Germany, June 17-23, 2002 [hep-ph/0212227].
12. D. Hooper and T. Plehn, Phys. Lett. **B562**, 18 (2003).
13. R. Bernabei *et al.*, Riv. N. Cim. **26** n. 1 (2003) 1.
14. P. Belli, R. Cerulli, N. Fornengo and S. Scopel, Phys. Rev. D **66**, 043503 (2002).
15. D.S. Akerib *et al.*, Phys. Rev. Lett. **93** (2004) 211301.
16. A. Benoit *et al.*, Phys. Lett. B **545**, 43 (2002).
17. A. Habig [Super-Kamiokande Collaboration], *Proceedings of the 27th International Cosmic Ray Conferences (ICRC 2001)*, Hamburg, Germany, August 7-15, 2001 [hep-ex/0106024].
18. M. Ambrosio *et al.* [MACRO Collaboration], Phys. Rev. D **60**, 082002 (1999).
19. X. Bai *et al.* [AMANDA Collaboration], *Proceedings of the 28th International Cosmic Ray Conferences (ICRC 2003)*, Tsukuba, Japan, 31 Jul - 7 Aug 2003.
20. M.M. Boliev *et al.*, *Proceedings of the International Workshop on Aspects of Dark Matter in Astrophysics and Particle Physics, Heidelberg, Germany, 16-20 Sep 1996.*
21. S.D. Hunter *et al.*, Astrophys. J. **481**, 205 (1997).
22. J.F. Navarro, C.S. Frenk and S.D.M. White, Astrophys. J. **462**, 563 (1996).
23. B. Moore et al., Mon. Not. Roy. Astron. Soc. **310**, 1147 (1999).

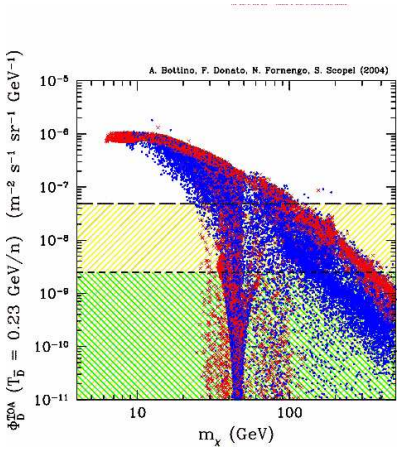

Fig. 7. Scatter plot of the antideuteron flux at kinetic energy $T_{\bar{p}} = 0.23$ GeV$/n$ as a function of the neutralino mass. A spherical isothermal dark matter density profile has been used. The solar modulation is calculated at the phase of solar minimum. Crosses (red) and dots (blue) denote neutralino configurations with $0.095 \leq \Omega_\chi h^2 \leq 0.131$ and $\Omega_\chi h^2 < 0.095$, respectively. The shaded region denotes the estimated sensitivity [24] to low–energy antideuterons for the AMS experiment [29] on borad of the International Space Station. The hatched region shows the estimated sensitivity for the proposed GAPS antideuteron experiment [30].

24. F. Donato, N. Fornengo, and P. Salati, Phys. Rev. D **62**, 043003 (2000).
25. F. Donato, N. Fornengo, D. Maurin, P. Salati, R. Taillet, Phys. Rev. D **69**, 063501 (2003).
26. S. Orito, *et al.* (BESS Collaboration), Phys. Rev. Lett. **84**, 1078 (2000).
27. T. Maeno, *et al.* (BESS Collaboration), Astropart. Phys. **16**, 121 (2001).
28. F. Donato *et al.*, Astrophys. J. **563**, 172 (2001).
29. S. Ahlen *et al.*, Nucl. Inst. Meth. **A350**, 351 (1994).
30. K. Mori *et al.* Ap. J. **566**, 604 (2002).